Published in final edited form as:
Acta Biomater. 2012 December ; 8(12): 4397–4404. doi:10.1016/j.actbio.2012.07.048.

Influence of select extracellular matrix proteins on mesenchymal stem cell osteogenic commitment in 3D contexts

Silvia Becerra-Bayona, BS[1], **Viviana Guiza-Arguello, BS**[2,†], **Xin Qu, PhD**[2,†], **Dany Munoz-Pinto, PhD**[2], and **Mariah S. Hahn, PhD**[1,2,3,*]

[1]Materials Science and Engineering Program, Texas A&M University, College Station, TX

[2]Department of Chemical Engineering, Texas A&M University, College Station, TX

[3]Department of Biomedical Engineering, Texas A&M University, College Station, TX

Abstract

Growth factors have been shown to be powerful mediators of mesenchymal stem cell (MSC) osteogenic differentiation. However, their use in tissue engineered scaffolds not only can be costly but also can induce undesired responses in surrounding tissues. Thus, the ability to specifically promote MSC osteogenic differentiation in the absence of exogenous growth factors via manipulation of scaffold material properties would be beneficial. The current work examines the influence of select extracellular matrix (ECM) proteins on MSC osteogenesis toward the goal of developing scaffolds with intrinsically osteoinductive properties. Fibrinogen (FG), fibronectin (FN), and laminin-1 (LN) were chosen for evaluation due to their known roles in bone morphogenesis or bone fracture healing. These proteins were conjugated into poly(ethylene glycol) diacrylate (PEGDA) hydrogels and their effects on encapsulated 10T½ MSCs were evaluated. Specifically, following 1 week of culture, mid-term markers of various MSC lineages were examined in order to assess the strength and specificity of the observed osteogenic responses. PEG-LN gels demonstrated increased levels of the osteogenic transcription factor osterix relative to day 0 levels. In addition, PEG-FG and PEG-LN gels were associated with increased deposition of bone ECM protein osteocalcin relative to PEG-FN gels and day 0. Importantly, the osteogenic response associated with FG and LN appeared to be specific in that markers for chondrocytic, smooth muscle cell, and adipocytic lineages were not similarly elevated relative to day 0 in these gels. To gain insight into the integrin dynamics underlying the observed differentiation results, initial integrin adhesion and temporal alterations in cell integrin profiles were evaluated. The associated results suggest that α_2, α_v, and α_6 integrin subunits may play key roles in integrin-mediated osteogenesis.

INTRODUCTION

Mesenchymal stem cells (MSCs) are being increasingly recognized as a viable cell source for bone regeneration applications due to their ability to be expanded in vitro and to differentiate into a number of cell lineages. MSC differentiation is known to be influenced

*Corresponding Author: Mariah S Hahn, PhD, Texas A&M University, Department of Chemical Engineering, Telephone: 979-739-1343, Fax: 979-845-6446, mhahn@tamu.edu.
†Viviana Guiza-Arguello and Xin Qu contributed equally to this work.

by a range of environmental stimuli, among the most potent of which are growth factors. However, the use of exogenous growth factors in tissue engineering scaffolds not only can be costly but also can induce undesired responses in surrounding tissues. Thus, MSC-based bone regeneration strategies would be benefited by the identification of scaffold material properties which intrinsically promote osteoblast lineage progression in the absence of exogenous growth factors.

A number of 2D studies have demonstrated MSC osteogenic differentiation to be tightly regulated by cellular interactions with the surrounding extracellular matrix (ECM) [1–13]. However, comparatively little is known regarding the effects of various ECM components in regulating MSC osteogenesis in 3D scaffold environments [14–16]. This is significant since recent studies suggest that effects observed in 2D may not be indicative of the effects of the same scaffold variables in more biomimetic 3D culture systems [17–19]. Therefore, the current work focuses on elucidating the influence of select ECM constituents on MSC osteogenic differentiation in 3D contexts.

Towards this goal, we incorporated specific ECM molecules into hydrogel scaffolds designed to have moduli within the “osteogenic” range identified in the 3D human and mouse MSC studies of Huebsch et al. [20]. In selecting molecules for examination, we chose to focus on several ECM proteins associated with bone morphogenesis (fibronectin [21] and laminin-1 [22, 23]) or bone fracture healing (fibrinogen [24]). These proteins were then conjugated into poly(ethylene glycol) diacrylate (PEGDA) hydrogel networks. PEGDA hydrogels were selected as the base scaffold due to the broad tunability of their mechanical properties and their previous use in bone regeneration applications [25–28]. In addition, pure PEGDA hydrogels function as biological “blank slates” in that they do not significantly adsorb cell adhesive serum proteins and therefore do not intrinsically promote cell adhesion [29]. Thus, cell interactions with PEGDA gels are initially isolated to the proteins specifically tethered to the scaffold as well as the interactions supported by these proteins (e.g. growth factor binding).

In the present study, 10T½ MSCs were encapsulated within PEGDA hydrogels containing defined amounts of fibronectin (FN), fibrinogen (FG) or laminin-1 (LN). The levels of various markers of osteoblast, chondrocytic, smooth muscle cell, and adipocytic fates were then monitored with time in culture toward assessing the strength and specificity of observed osteogenic responses. Due to the critical role of integrins in transducing the signals provided by glycoproteins such as FN, FG, and LN [30], initial integrin adhesion profiles as well as temporal alterations in cell integrin profiles were also characterized.

MATERIAL AND METHODS

Polymer Synthesis and Characterization

PEG-Diacrylate Synthesis—PEGDA was prepared as previously described [31] by combining 0.1 mmol/ml dry PEG (10 kDa, Fluka), 0.4 mmol/ml acryloyl chloride, and 0.2 mmol/ml triethylamine in anhydrous dichloromethane and stirring under argon overnight. The resulting solution was washed with 2 M K_2CO_3 and separated into aqueous and dichloromethane phases to remove HCl. The organic phase was subsequently dried with anhydrous $MgSO_4$, and PEGDA was precipitated in diethyl ether, filtered, and dried under vacuum. Acrylation of the PEG end hydroxyl groups was characterized by ^{1}H-NMR to be ~95%.

Synthesis of Acrylate-Derivatized Proteins—Proteins FN (human plasma, BD Biosciences), FG (human plasma, Sigma Aldrich), and LN (mouse, BD Biosciences) were lightly functionalized in their folded state by reaction with acryloyl-PEG-N-

hydroxysuccinimide (ACRL-PEG-NHS, 3.4 kDa, Nektar) at a 1:2 molar ratio at pH 8.5 [31]. The resulting acrylate-derivatized products were purified by dialysis against a 100 kDa membrane, lyophilized, and stored at −20 °C until use. ACRL-PEG conjugation to the target proteins was confirmed using ^{1}H-NMR. A representative ^{1}H-NMR spectrum for acrylate-derivatized FG is shown in Supplementary Figure 1.

To confirm the ability of the modified proteins to be incorporated within PEGDA hydrogel networks, hydrogel precursor solutions were prepared with 0.5 mg/mL protein and 100 mg/mL PEGDA. Following addition of 10 μL/mL of a 300 mg/mL solution of UV photoinitiator 2,2-dimethoxy-2-phenyl-acetophenone (DMAP) in N-vinylpyrrolidone (NVP), gels were polymerized by 4 min exposure to longwave UV light (Spectroline, ~6 mW/cm^2, 365 nm). The gels were then immersed in PBS overnight, after which they were transferred to a 0.1 NaOH solution to hydrolyze the PEGDA crosslinks and release encapsulated protein. The levels of protein released were compared to the levels in the precursor solution using the CBQCA assay (Invitrogen), and the average level of protein incorporation was found to be consistent across protein types at 86.7 ± 7.2%. In addition, to assess the ability of cells to interact with proteins incorporated into the hydrogel network, 10T½ cells were seeded onto the surface of each gel formulation. Cell adhesion and spreading were confirmed for each PEG-ECM gel type (Supplementary Figure 2).

Cell Culture, Initial Characterization, and Encapsulation

Cryopreserved 10T½ mouse MSCs (American Type Culture Collection; ATCC) at passage 2 were thawed and expanded in monolayer culture per ATCC protocols. Prior to encapsulation, cells were maintained at 37 °C and 5% CO_2 in Dulbecco's Modified Eagle's Media (DMEM, Hyclone) supplemented with 10% heat-inactivated fetal bovine serum (FBS, Hyclone). Cells at passage 4–6 were termed "day 0" and were harvested and allocated for either protein extraction, integrin blocking studies, or hydrogel encapsulation.

Protein Extraction—Proteins were extracted from day 0 10T½ cells by the addition of Trizol (Invitrogen) per manufacture's protocols. The resulting solutions were centrifuged, and each supernatant was mixed with chloroform (Sigma), vigorously shaken for 15 s, and centrifuged. The lower protein-rich phenol-chloroform phase of each sample (n = 4) was mixed with ethanol to precipitate residual DNA. The resulting phenol-ethanol phase was transferred to a 3.4 kDa SnakeSkin dialysis membrane (Pierce). The solution was dialyzed for ~60 h at 4 °C against an aqueous solution of 0.1% sodium dodecyl sulfate (SDS), with buffer exchange every ~18 h. By the end of the third 18 h dialysis period, the samples had partitioned into three phases: (1) a supernatant, (2) a globular mass, and (3) a colorless, viscous liquid. The globular mass, containing the bulk of sample proteins [32], was resuspended in PBS containing 0.5% SDS and 1% Triton X-100. The isolated sample proteins were subsequently used in quantitative ELISA assays.

Integrin Blocking Studies—Standard adhesion blocking studies were performed to determine the integrin alpha subunits through which the 10T½ cells initially interacted with the PEG-ECM gels. In brief, functionalized FG, FN, and LN were resuspended in PBS at 100 μg/mL, after which they were applied to a 96 well, high protein binding plate at 100 μl/well for 12 h at 4 °C. The wells were then blocked with 3% bovine serum albumin (BSA). Harvested 10T½ cells were washed with PBS and resuspended in serum-free DMEM supplemented with 1 mM Ca^{2+} and Mg^{2+}. Cells were then exposed to 50 μg/mL of α_1, α_2, α_5, α_v, or α_6 integrin antibodies or to 50 μg/mL of appropriate negative control antibodies for 30 min at room temperature. Further details regarding antibodies are given in Supplementary Table 1. The cell suspensions were subsequently applied to the coated wells at 10,000 cells/cm^2. Following 30 min incubation at 37 °C and 5% CO_2, wells were rinsed 3

times with PBS. Adherent cells were then lysed, and the number of adherent cells in each well was measured using a lactate dehydrogenase assay kit (Roche). Percent inhibition was evaluated relative to the corresponding negative control. At least 5 sample wells per antibody were analyzed for each protein type.

Cell Encapsulation and Culture—Hydrogels were fabricated by preparing: 1.) a 20 wt % PEGDA solution in HEPES-buffered saline (HBS) and 2.) separate solutions of 1 mg/mL acrylate-derivatized FN, FG, or LN in HBS. A 300 mg/ml solution of DMAP in NVP was added at 2 (v/v)% to the PEGDA mixture. The PEGDA and protein solutions were then separately sterilized by filtration, after which each protein solution was mixed with an equal volume of the 20 wt% PEGDA solution. Harvested 10T½ cells were resuspended in the resulting precursor solutions at 1×10^6 cells/mL. The cell suspensions were then pipetted into molds composed of two glass plates separated by 0.5 mm polycarbonate spacers and polymerized by 4 min exposure to longwave UV light (Spectroline, ~6 mW/cm^2, 365 nm). A set of the resulting hydrogels were harvested for “day 0” analyses as described in the following section. Remaining hydrogel slabs were transferred to Omnitrays (Nunc) fitted with 4 sterile polycarbonate bars to simultaneously prevent gel flotation and prevent gel contact with the tray bottom. Hydrogels were immersed in DMEM supplemented with 10% FBS, 100 U/mL penicillin, and 100 mg/L streptomycin and maintained at 37 °C and 5% CO_2. Media was changed every two days.

Day 0 Hydrogel Characterization

Average Mesh Size—PEGDA hydrogel mesh structure cannot be visualized using standard techniques such as scanning electron microscopy. In the present study, average hydrogel mesh size was therefore characterized via a series of dextran diffusion experiments based on an adaptation of the methodology of Watkins et al [33]. In brief, samples were collected from the freshly prepared PEG-ECM hydrogels and allowed to swell overnight at 37 °C in PBS containing 0.05% azide (PBS-azide). Eight-mm diameter discs were then harvested from each gel formulation, and solutions containing 0.05 mg/mL fluorescently-labeled dextran (10 kDa, Invitrogen) in PBS-azide were added at 1 mL per hydrogel disc. Dextran solutions were allowed to diffuse into the hydrogels for 24 h at 37 °C. Each gel disc was then gently blotted and transferred to 1 mL fresh PBS-azide. Dextran that had penetrated into the hydrogels was then permitted to diffuse out into the surrounding solution at 37 °C. After 24 h, the fluorescence of the PBS-azide solution surrounding each disc was measured at ex/em 488/532. Dextran standard curves were used to convert each fluorescence signal to a concentration. For each hydrogel, the measured dextran concentration was divided by gel weight [34]. The resulting value served as a quantitative indicator of hydrogel permissivity.

Hydrogel Mechanical Properties—Samples were collected from each freshly prepared hydrogel formulation and allowed to swell overnight in PBS-azide. Eight-mm discs (n = 4 per formulation) were then cored from each gel sample and mechanically tested under unconfined compression using a DMA 800 (TA Instruments). Following application of a 0.01 N preload, each disc was subjected to compression at a rate of 0.1 mm/min. The compressive modulus of each hydrogel was extracted from the resulting stress-strain data over a 10–25% strain range.

Cell Density—Samples (n = 4) were collected from each freshly prepared hydrogel formulation following 24 h immersion in culture media. Hydrogel samples were digested for 72 h at 37 °C in 1 ml of 0.12 M NaOH per 0.2 g hydrogel wet weight [35, 36]. Aliquots of the hydrolyzed samples were neutralized, and their DNA content determined using the Invitrogen PicoGreen assay [37]. DNA measures were translated to cell number using a

conversion factor of 6.6 pg DNA per cell [38]. Calf thymus DNA (Sigma) subjected to the same association with PEGDA and to the same digestion conditions as the samples served as a standard.

Endpoint Analyses

At day 7 of culture, samples were harvested from each hydrogel formulation for mechanical, mesh size, DNA, ELISA, and histological analyses. Samples collected for histological analyses (n = 4–8 per formulation) were fixed in 10% formalin for 30 min and embedded in Tissue-Tek freezing medium. Samples harvested for mechanical (n = 4 per formulation), mesh size (n = 4 per formulation), and DNA (n = 4 per formulation) assessments were evaluated according to the same protocols as the day 0 specimens. Similarly, samples harvested for ELISA analyses (n = 6–9 per formulation) were homogenized in Trizol using a Bead-Beater homogenizer (Biospec), after which sample proteins were isolated as described for day 0 specimens.

ELISA Analyses—Proteins extracted from the day 0 cells and the day 7 constructs were evaluated for mid-term differentiation markers and various integrin alpha subunits via competitive ELISAs. Further details regarding the antibodies employed are given in Supplementary Table 1. For each antibody examined, high binding EIA 96 well plates (Costar) were coated overnight at 4 C with appropriate competitive peptide. The concentration of applied competitive peptide was 200 ng/well, except for β-actin (50 ng/well). The coated wells were then blocked with BSA and rinsed with PBS. Aliquots of each sample were incubated with primary antibody for 1 h, after which the sample-antibody mixtures were applied to coated wells for 1 h. Standard curves were similarly prepared by incubating primary antibody with varying levels of competitive peptide for 1 h, followed by solution application to coated wells. For both samples and standards, primary antibody which had bound to the coated wells was detected using an appropriate HRP-conjugated secondary antibody (Jackson Immunoresearch), followed by application of 2,2'-azino-bis(3-ethylbenzthiazoline-6-sulphonic acid) (Sigma) and monitoring of absorbance at 410 nm. Each target protein was analyzed in duplicate for each sample (n = 6–9 per day 7 gel type; n = 4 for day 0) and normalized to the housekeeping protein β-actin.

Histological Analyses—Bone ECM deposition (osteopontin and osteocalcin) was further analyzed using standard immunohistochemical technique. In brief, 35 μm sections were cut from each embedded histological sample (n = 4–8 per formulation) using a cryomicrotome. Rehydrated sections were blocked with peroxidase for 30 min followed by 30 min exposure to Terminator (Biocare Medical). Primary antibodies for osteopontin and osteocalcin were diluted in PBS containing 3% BSA and then applied to the sections for 1 h. Bound primary antibody was detected using HRP-conjugated secondary antibody (Jackson Immunoresearch) followed by application of chromogens AEC (LabVision) or DAB (Biocare Medical). For detection of intracellular differentiation markers (myocardin and PPAR), rehydrated sections were permeabilized (10 mM HEPES, pH 6.8, 100 mM NaCl, 3mM $MgCl_2$, 300 mM sucrose, 0.5% Triton X-100) for 30 min prior to Terminator application. Further details regarding the antibodies employed are given in Supplementary Table 1.

Stained sections were imaged using a Zeiss Axiovert microscope, and cell counts were carried out to semi-quantitatively evaluate immunostaining results for intracellular markers myocardin and PPAR. These counting assessments were conducted according to established methods [25, 39, 40] on sections from each sample (n = 4–8 per gel formulation). For each cell, i, in a given section, a single observer blinded to outcome assigned a staining intensity, d_i, on a scale of 0–3 (0 = “no staining” and 3 = “highest intensity among all formulations for

that antibody"). The cumulative staining intensity, d, for a given antibody in a particular section was calculated using the following equation: $d = (d_i)/(\text{total cell number})$. In addition, since deposited ECM remained localized around the parent cells in each hydrogel formulation, as is characteristic for PEGDA gels [41], the relative levels of osteocalcin and osteopontin among hydrogel formulations were also evaluated by cell counts per the above procedure. Osteocalcin counts were used to internally validate the counting approach by direct comparison with corresponding quantitative ELISA data (Supplementary Figure 3). The degree of correlation between the two assessment techniques was 98.9% by Pearson's correlation coefficient method.

Statistical Analyses

Data are reported as mean ± standard deviation. Comparison of sample means was performed by ANOVA followed by Tukey's post-hoc test (SPSS software), $p < 0.05$.

RESULTS

Hydrogel Material Properties and Cell Density

A range of scaffold properties, including modulus, permeability, and degradation rate, have been found to impact MSC lineage progression. Therefore, in order to attribute differences in 10T½ cell behavior across hydrogel formulations specifically to initial differences in gel protein composition, it was important that the remaining hydrogel material properties could be considered consistent across gels. Hydrogels formed from pure PEGDA degrade slowly (over a period of 1–2 years) and resist cell-mediated gel contraction, ensuring consistent bulk gel properties over a broad time range [36, 37, 42–44]. In the present study, a 200:1 weight ratio of PEGDA to protein was therefore selected to ensure that the network properties of the resulting gels would be dominated by PEGDA. To confirm this, the modulus, mesh size, thickness, and mass of the PEG-ECM hydrogels were characterized both at day 0 and day 7.

As shown in Table 1, the initial elastic moduli of the PEG-FG, PEG-FN, and PEG-LN gels were similar at approximately 33 kPa. Importantly, each of these initial moduli were within the osteogenic range identified by the 3D studies of Huebsch et al. [20]. To assess degradation and cell-mediated contraction, hydrogel modulus and thickness were evaluated across time in culture. Comparison of initial and endpoint mechanical data indicated that, although modulus decreased by approximately 15% over the 7 day culture time for each gel formulation, hydrogel modulus remained consistent across formulations (Table 1). Similarly, average mesh size was consistent across hydrogels at both day 0 to day 7 (Table 1). The initial and endpoint thickness data for 8 mm gel discs indicated a negligible alteration in gel volume with time. In addition, net cell proliferation and loss was examined for each PEG-ECM hydrogel over the 7 day culture period. The cell density in each PEG-ECM hydrogel following 7 days of culture was between 78–86% of the initial seeding density (Table 2), consistent with PEG hydrogel literature [15, 27, 39, 45–47]. Combined, the above data indicate that: 1.) each hydrogel formulation maintained an osteogenic modulus throughout the study [20] and 2.) differences in cell responses among formulations can be attributed to differences in the initial proteins tethered to the gel network, their interactions with other molecules, and subsequent neo-matrix deposition.

Cell Differentiation

Following 7 days of culture, cell differentiation was examined by quantitative ELISA or by cell counts (as validated in Supplementary Figure 3). As shown in Figure 1, day 7 levels of various osteogenic markers indicated significant differences relative to day 0 and/or among hydrogel formulations. Specifically, cells in PEG-LN gels expressed significantly higher

levels of the osteogenic transcription factor osterix than day 0 cells ($p = 0.032$), while osterix expression in PEG-FN gels could not be distinguished from day 0 levels. In addition, PEG-LN gels retained day 0 osteopontin expression levels, whereas osteopontin levels in day 7 PEG-FN gels had fallen to approximately half of day 0 levels ($p = 0.005$). Similarly, day 7 PEG-FN gels contained significantly lower levels of the bone ECM protein osteocalcin relative to PEG-FG ($p = 0.042$) and PEG-LN ($p = 0.002$) gels, whereas PEG-FG and PEG-LN gels contained 2.4- and 2.9-fold greater osteocalcin levels than day 0 ($p = 0.004$ and $p < 0.001$, respectively).

To assess the specificity of the osteogenic response associated with the PEG-FG and PEG-LN gels, mid-term markers of chondrogenesis, smooth muscle progression, and adipogenesis were evaluated (Figure 2). Day 7 expression of smooth muscle transcription factor myocardin was similar to day 0 levels and across hydrogel formulations. In addition, day 7 levels of SM22α, a cytoskeletal protein associated with smooth muscle differentiation, could also not be distinguished among gel formulations or from day 0 levels. PPAR expression was consistently similar to day 0 levels across the day 7 gels, and the day 7 levels of the adipocyte intracellular protein A-FABP were statistically indistinguishable from day 0 levels and among formulations. Furthermore, day 7 expression of chondrogenic transcription factor sox9 did not vary significantly with gel formulation or relative to day 0, and day 7 levels of the cartilage-associated ECM protein collagen II could also not be distinguished among the PEG-ECM gels or relative to day 0. Representative immunostaining images for proteins evaluated by cell counts (myocardin, PPAR, and osteopontin) are given in Figure 3.

Integrin Expression

Integrin-associated signaling has been demonstrated to play a key role in MSC osteogenic lineage progression [1–3, 8, 9, 12]. Therefore, initial integrin adhesion and temporal alterations in cell integrin profiles were evaluated in order to gain insight into the integrin dynamics underlying the observed differentiation results.

Initial Integrin Adhesion—Inhibition studies were conducted to characterize the integrins through which cells initially interacted with the various PEG-ECM hydrogels. As illustrated in Table 3, the day 0 population of 10T½ cells interacted with each PEG-ECM gel via a distinct panel of integrins. Specifically, cell adhesion to functionalized FG was inhibited by antibodies to α_v and α_5 integrin subunits, although integrin α_v appeared to be dominant. In contrast, cell binding to FN was significantly inhibited by antibodies to α_2, α_v, and α_5 integrin subunits, whereas LN interacted with α_1, α_v, α_5, and α_6 integrin subunits.

Endpoint Integrin Profiles—To investigate potential temporal alterations in cell-substrate integrin interactions, endpoint expression of various integrins was investigated relative to day 0. Day 7 expression of integrin subunits α_1, α_v, and α_5 did not significantly vary among PEG-ECM gels or relative to day 0 levels (Figure 4). However, integrin α_2 expression was approximately 1.6-fold higher in day 7 PEG-LN gels than at day 0 ($p = 0.034$). Similarly, integrin α_6 expression in day 7 PEG-FG hydrogels was approximately 2-fold higher than at day 0 ($p = 0.030$) and was significantly greater than in PEG-FN gels ($p = 0.014$). Cumulatively, the endpoint integrin profiles associated with the PEG-FG and PEG-LN gels differed from their initial integrin profiles.

DISCUSSION

The aim of the present work was to compare the osteoinductivity of select ECM components in defined 3D environments toward the improved design of osteogenic scaffolds. To avoid the use of exogenous growth factors, these ECM components were examined within the

context of scaffolds with osteogenic moduli (~30 kPa) [20]. The associated temporal evolution in MSC lineage progression and integrin profiles were then characterized. Present data indicated that both FG and LN enhanced the osteogenic response of encapsulated 10T½ cells. Specifically, osteocalcin levels in day 7 PEG-FG and PEG-LN gels were approximately 2.4- and 2.9-fold greater, respectively, than day 0 levels. In addition, expression of osterix, an osteoblast-specific transcription factor required for osteogenesis, was significantly elevated in day 7 PEG-LN gels relative to day 0 levels. In contrast, the day 7 levels of markers for adipogenesis, chondrogenesis, and smooth muscle lineage progression were not significantly different among formulations or relative to day 0, indicating that the osteogenic response associated with the PEG-FG and PEG-LN gels was specific.

The present results are consistent with previous 2D studies demonstrating LN to support higher active levels of the osteogenic transcription factor Cbfα1 than FN over a 5 day culture time-frame [11]. In addition, a study by Salaszynk et al. indicated that, in the absence of osteogenic media supplements, FN did not support human MSC matrix mineralization, in contrast to collagen I and vitronectin [3]. Indeed, they found little role for FN in stimulating osteogenic differentiation [4], beyond activation of alkaline phosphatase [3]. Similarly, Benoit et al. found that FN increased alkaline phosphatase production, but not osteopontin gene expression [15]. Although fibrin glue has been used extensively in bone tissue engineering [24, 48–58], literature presents conflicting reports regarding the osteoinductivity of fibrinogen. Specifically, while several studies have suggested that fibrin sealants promote osteogenesis [51, 53–55], other studies have reported negative effects when fibrin sealants were combined with coral granules [57, 58] and poly(lactide-co-glycolic acid) scaffolds [56]. These conflicting results may arise, in part, from differences in the material properties of the various fibrin-containing scaffolds assayed. In the present study, we tightly controlled initial scaffold material properties as well as the temporal evolution of those properties in order to isolate the osteoinductive effect of FG from other matrix properties.

To gain insight into the origins of the osteogenic response associated with FG and LN, we examined the initial integrin-based interactions supported by these ECM components. Specifically, integrin blocking studies indicated that day 0 10T½ cells interacted with FG primarily through α_v integrin subunits. MSC-matrix interactions through α_v subunits have previously been correlated with osteoinductivity [3, 59]. In particular, Salaszynk et al. found that human MSCs bound to vitronectin primarily (> 90% of adhesive interactions) through α_v subunits, and that vitronectin was capable of promoting osteogenic differentiation, even in the absence of added growth factors [3]. Similarly, Connelly et al. [59] and Yang et al. [28] demonstrated that the peptide RGD, which primarily supports α_v interactions, promoted expression of osteocalcin.

In contrast to FG, day 0 10T½ cells bound to FN through integrins α_2, α_v, and α_5. As with integrin α_v, the α_2 subunit has been associated with osteogenic differentiation in the case of both MSCs [1, 60] and pre-osteoblasts [8]. Specifically, Shih et al. found that increased MSC osteogenesis was linked to an increase in integrin α_2 expression, and that knockdown of integrin α_2 downregulated osteogenic differentiation markers [60]. In addition, anti-α_2 integrin antibody was found to block ascorbic acid dependent induction of alkaline phosphatase [13] and of the osteocalcin promoter [8] in MC3T3-E1 pre-osteoblasts. In contrast to integrin α_2, studies involving human MSCs suggest that integrin α_5 interactions do not support osteogenesis in the absence of osteoinductive media supplements [3]. Thus, the reduced osteogenic response associated with PEG-FN gels may be due, in part, to integrin α_5 signaling dominating over or interfering with pro-osteogenic integrin α_2 and α_v signals. That said, it is interesting to note that, in the presence of osteogenic media supplements, integrin α_5 interactions have been found to support osteogenesis [20].

As for FN, day 0 10T½ interactions with LN were mediated by both integrins α_v and α_5. However, LN also supported significant levels of integrin α_1 and α_6 interactions. As with integrins α_2 and α_v, integrins α_1 and α_6 have previously been associated with osteogenesis. In particular, Gronthos et al. found that incubating pre-osteoblasts with a function blocking antibody against integrin α_1 inhibited matrix mineralization [61]. In addition, Salaszynk et al. found that collagen I-coated surfaces stimulated human MSC matrix mineralization, and that cell interactions with these surfaces were initially mediated primarily by α_1 subunits (> 90% of adhesive interactions) [3]. Similarly, integrin α_6 upregulation has been associated with the MSC osteogenic responses observed on rough titanium surfaces [62, 63] and poly(lactide-co-glycolide) constructs [64]. Thus, the osteoinductive effect associated with PEG-LN gels may arise, in part, from integrin α_1, α_v, and α_6 interactions predominating over integrin α_5 interactions.

The osteoinductive role for integrins α_2 and α_6 noted in literature was further supported by the temporal variations in integrin profiles observed in the present study. Specifically, PEG-FG gels were associated with an increase in integrin α_6 expression over the time-course of the study, and PEG-LN gels were associated with an increase in integrin α_2 expression. The increased expression of these integrin subunits may therefore have contributed to the osteogenic effects of both the PEG-LN and PEG-FG gels, although definitive statements cannot be made since the presence of a specific integrin does not necessarily imply its activity.

Several limitations of the present study merit comment. FG, FN, and LN each support an array of interactions, such as cytokine and ECM protein binding, which likely influenced both integrin-mediated and non-integrin mediated cell-hydrogel interactions. In addition, non-integrin cell-ECM interactions associated with deposited neo-matrix (e.g. cell-growth factor interactions) were not assessed. Thus, the present interpretations linking osteogenic responses to particular integrins must be treated with caution. In particular, further studies would be required to establish potential causative relationships between observed cell responses and associated integrin profiles. Finally, osteogenesis represents a complex set of processes that are mediated by a number of factors. The interplay between these factors and the precise sequences leading to osteogenic commitment are not fully understood, and the present study examined only a limited subset of the interactions and a limited panel of markers that characterize osteogenesis. In addition, the present study was conducted using cells derived from the mouse embryonic mesoderm. Although these cells demonstrate multipotency, their responses may not be indicative of the behavior of adult human mesenchymal stem cells. Furthermore, the present results do not enable the impact of the 3D culture environment itself to be assessed.

Despite these limitations, the cumulative ECM and phenotypic data indicate that LN may be the most appropriate of the biomolecules examined for promoting specific osteogenic differentiation within the context of scaffolds with osteoinductive moduli. Future studies will focus on exploring a broader range of time points and ECM protein concentrations as well as on examining potential synergy between various ECM components.

Supplementary Material

Refer to Web version on PubMed Central for supplementary material.

Acknowledgments

We would like to acknowledge the NSF DMR CAREER Award for funding.

REFERENCES

1. Kundu AK, Putnam AJ. Vitronectin and collagen I differentially regulate osteogenesis in mesenchymal stem cells. Biochemical and Biophysical Research Communications. 2006; 347:347–357. [PubMed: 16815299]
2. Kundu AK, Khatiwala CB, Putnam AJ. Extracellular matrix remodeling, integrin expression, and downstream signaling pathways influence the osteogenic differentiation of mesenchymal stem cells on poly(lactide-co-glycolide) substrates. Tissue Engineering Part A. 2009; 15:273–283. [PubMed: 18767971]
3. Salasznyk R, Williams W, Boskey A, Batorsky A, Plopper G. Adhesion to vitronectin and collagen I promotes osteogenic differentiation of human mesenchymal stem cells. J Biomed Biotechnol. 2004; 2004:24–34. [PubMed: 15123885]
4. Klees R, Salasznyk R, Kingsley K, Williams W, Boskey A, Plopper G. Laminin-5 induces osteogenic gene expression in human mesenchymal stem cells through an ERK dependent pathway. Mol Biol Cell. 2005; 16:881–890. [PubMed: 15574877]
5. Klees RF, Salasznyk RM, Vandenberg S, Bennett K, Plopper GE. Laminin-5 activates extracellular matrix production and osteogenic gene focusing in human mesenchymal stem cells. Matrix Biology. 2007; 26:106–114. [PubMed: 17137774]
6. Salasznyk R, Klees R, Hughlock M, Plopper G. ERK signaling pathways regulate the osteogenic differentiation of human mesenchymal stem cells on collagen I and vitronectin. Cell Commun Adhes. 2004; 11:137–153. [PubMed: 16194881]
7. Xiao G, Gopalakrishnan R, Jiang D, Reith E, Benson M, Franceschi R. Bone morphogenetic proteins, extracellular matrix, and mitogen-activated protein kinase signaling pathways are required for osteoblast-specific gene expression and differentiation in MC3T3-E1 cells. J Bone Miner Res. 2002; 17:101–110. [PubMed: 11771655]
8. Xiao G, Wang D, Benson M, Karsenty G, Franceschi R. Role of the alpha2-integrin in osteoblast-specific gene expression and activation of the Osf2 transcription factor. J Biol Chem. 1998; 273:32988–32994. [PubMed: 9830051]
9. Salasznyk RM, Klees RF, Boskey A, Plopper GE. Activation of FAK is necessary for the osteogenic differentiation of human mesenchymal stem cells on laminin-5. J Cell Biochem. 2007; 100:499–514. [PubMed: 16927379]
10. Klees RF, Salasznyk RM, Ward DF, Crone DE, Williams WA, Harris MP, et al. Dissection of the osteogenic effects of laminin-332 utilizing specific LG domains: LG3 induces osteogenic differentiation, but not mineralization. Experimental Cell Research. 2008; 314:763–773. [PubMed: 18206871]
11. Huang C-H, Chen M-H, Young T-H, Jeng J-H, Chen Y-J. Interactive effects of mechanical stretching and extracellular matrix proteins on initiating osteogenic differentiation of human mesenchymal stem cells. J Cell Biochem. 2009; 108:1263–1273. [PubMed: 19795386]
12. Salasznyk RM, Klees RF, Williams WA, Boskey A, Plopper GE. Focal adhesion kinase signaling pathways regulate the osteogenic differentiation of human mesenchymal stem cells. Experimental Cell Research. 2007; 313:22–37. [PubMed: 17081517]
13. Takeuchi Y, Nakayama K, Matsumoto T. Differentiation and cell surface expression of transforming growth factor-beta receptors are regulated by interaction with matrix collagen in murine osteoblastic cells. J Biol Chem. 1996; 271:3938–3944. [PubMed: 8632016]
14. Lund AW, Stegemann JP, Plopper GE. Inhibition of ERK promotes collagen gel compaction and fibrillogenesis to amplify the osteogenesis of human mesenchymal stem cells in three-dimensional collagen I culture. Stem Cells and Development. 2009; 18:331–342. [PubMed: 18491946]
15. Benoit DSW, Durney AR, Anseth KS. The effect of heparin-functionalized PEG hydrogels on three-dimensional human mesenchymal stem cell osteogenic differentiation. Biomaterials. 2007; 28:66–77. [PubMed: 16963119]
16. Hwang NS, Varghese S, Li H, Elisseeff J. Regulation of osteogenic and chondrogenic differentiation of mesenchymal stem cells in PEG-ECM hydrogels. Cell Tissue Res. 2011; 344:499–509. Epub 2011 Apr 19. [PubMed: 21503601]

17. Parekh SH, Chatterjee K, Lin-Gibson S, Moore NM, Cicerone MT, Young MF, et al. Modulus-driven differentiation of marrow stromal cells in 3D scaffolds that is independent of myosin-based cytoskeletal tension. Biomaterials. 2011; 32:2256–2264. [PubMed: 21176956]
18. Cukierman E, Pankov R, Stevens DR, Yamada KM. Taking Cell-Matrix Adhesions to the Third Dimension. Science. 2001; 294:1708–1712. [PubMed: 11721053]
19. Bissell MJ, Rizki A, Mian IS. Tissue architecture: the ultimate regulator of breast epithelial function. Curr Opin Cell Biol. 2003; 15:753–762. [PubMed: 14644202]
20. Huebsch N, Arany PR, Mao AS, Shvartsman D, Ali OA, Bencherif SA, et al. Harnessing traction-mediated manipulation of the cell/matrix interface to control stem-cell fate. Nat Mater. 2010; 9:518–526. [PubMed: 20418863]
21. Weiss RE, Reddi AH. Appearance of fibronectin during the differentiation of cartilage, bone, and bone marrow. The Journal of Cell Biology. 1981; 88:630–636. [PubMed: 7217207]
22. Foidart J-M, Reddi AH. Immunofluorescent localization of type IV collagen and laminin during endochondral bone differentiation and regulation by pituitary growth hormone. Developmental Biology. 1980; 75:130–136. [PubMed: 6154620]
23. Klotch DW, Ganey TM, Slater-Haase A, Sasse J. Assessment of bone formation during osteoneogenesis: A canine model. Otolaryngology - Head and Neck Surgery. 1995; 112:291–302. [PubMed: 7530832]
24. Bueno, E.; Glowacki, J. Biologic Foundations for Skeletal Tissue Engineering. Morgan and Claypool Publishers; 2011.
25. Benoit DSW, Schwartz MP, Durney AR, Anseth KS. Small functional groups for controlled differentiation of hydrogel-encapsulated human mesenchymal stem cells. Nat Mater. 2008; 7:816–823. [PubMed: 18724374]
26. Ayala R, Zhang C, Yang D, Hwang Y, Aung A, Shroff SS, et al. Engineering the cell-material interface for controlling stem cell adhesion, migration, and differentiation. Biomaterials. 2011; 32:3700–3711. [PubMed: 21396708]
27. Burdick JA, Anseth KS. Photoencapsulation of osteoblasts in injectable RGD-modified PEG hydrogels for bone tissue engineering. Biomaterials. 2002; 23:4315–4323. [PubMed: 12219821]
28. Yang F, Williams CG, Wang D-A, Lee H, Manson PN, Elisseeff J. The effect of incorporating RGD adhesive peptide in polyethylene glycol diacrylate hydrogel on osteogenesis of bone marrow stromal cells. Biomaterials. 2005; 26:5991–5998. [PubMed: 15878198]
29. Gombotz WR, Wang GH, Horbett TA, Hoffman AS. Protein adsorption to poly(ethylene oxide) surfaces. J Biomed Mater Res. 1991; 25:1547–1562. [PubMed: 1839026]
30. Humphries JD, Byron A, Humphries MJ. Integrin ligands at a glance. J Cell Sci. 2006; 119:3901–3903. [PubMed: 16988024]
31. Hahn MS, Miller JS, West JL. Laser scanning lithography for surface micropatterning on hydrogels. Advanced Materials. 2005; 17:2939–2942.
32. Hummon AB, Lim SR, Difilippantonio MJ, Ried T. Isolation and solubilization of proteins after TRIzol extraction of RNA and DNA from patient material following prolonged storage. Biotechniques. 2007; 42:467–472. [PubMed: 17489233]
33. Watkins AW, Anseth KS. Investigation of molecular transport and distributions in poly(ethylene glycol) hydrogels with confocal laser scanning microscopy. Macromolecules. 2005; 38:1326–1334.
34. Armstrong JK, Wenby RB, Meiselman HJ, Fisher TC. The hydrodynamic radii of macromolecules and their effect on red blood cell aggregation. Biophysical Journal. 2004; 87:4259–4270. [PubMed: 15361408]
35. Buxton AN, Zhu J, Marchant R, West JL, Yoo JU, Johnstone B. Design and characterization of poly(ethylene glycol) photopolymerizable semi-interpenetrating networks for chondrogenesis of human mesenchymal stem cells. Tissue Engineering. 2007; 13:2549–2560. [PubMed: 17655489]
36. Munoz-Pinto DJ, Jimenez-Vergara AC, Gelves LM, McMahon RE, Guiza-Arguello V, Hahn MS. Probing vocal fold fibroblast response to hyaluronan in 3D contexts. Biotechnology and Bioengineering. 2009; 104:821–831. [PubMed: 19718686]

37. Hahn MS, McHale MK, Wang E, Schmedlen RH, West JL. Physiologic pulsatile flow bioreactor conditioning of poly(ethylene glycol)-based tissue engineered vascular grafts. Annals of Biomedical Engineering. 2007; 35:190–200. [PubMed: 17180465]
38. Gregory TR. Nucleotypic effects without nuclei: Genome size and erythrocyte size in mammals. Genome. 2000; 43:895–901. [PubMed: 11081981]
39. Salinas CN, Anseth KS. The influence of the RGD peptide motif and its contextual presentation in PEG gels on human mesenchymal stem cell viability. Journal of Tissue Engineering and Regenerative Medicine. 2008; 2:296–304. [PubMed: 18512265]
40. Salinas CN, Anseth KS. The enhancement of chondrogenic differentiation of human mesenchymal stem cells by enzymatically regulated RGD functionalities. Biomaterials. 2008; 29:2370–2377. [PubMed: 18295878]
41. Liao H, Munoz-Pinto D, Qu X, Hou Y, Grunlan M, Hahn M. Influence of hydrogel material properties on vocal fold fibroblast extracellular matrix production and phenotype. Acta Biomateralia. 2008; 4:1161–1171.
42. Bryant SJ, Anseth KS. Controlling the spatial distribution of ECM components in degradable PEG hydrogels for tissue engineering cartilage. J Biomed Mater Res Part A. 2003; 64A:70–79.
43. Bryant SJ, Durand KL, Anseth KS. Manipulations in hydrogel chemistry control photoencapsulated chondrocyte behavior and their extracellular matrix production. J Biomed Mater Res Part A. 2003; 67A:1430–1436.
44. Peyton S, Raub C, Keschrumrus V, Putnam A. The use of poly(ethylene glycol) hydrogels to investigate the impact of ECM chemistry and mechanics on smooth muscle cells. Biomaterials. 2006; 27:4881–4893. [PubMed: 16762407]
45. Jimenez-Vergara AC, Munoz-Pinto DJ, Becerra-Bayona S, Wang B, Iacob A, Hahn MS. Influence of glycosaminoglycan identity on vocal fold fibroblast behavior. Acta Biomaterialia. 2011; 7:3964–3972. [PubMed: 21740987]
46. Steinmetz NJ, Bryant SJ. The effects of intermittent dynamic loading on chondrogenic and osteogenic differentiation of human marrow stromal cells encapsulated in RGD-modified poly(ethylene glycol) hydrogels. Acta Biomaterialia. 2011; 7:3829–3840. [PubMed: 21742067]
47. Nuttelman CR, Tripodi MC, Anseth KS. Synthetic hydrogel niches that promote hMSC viability. Matrix Biology. 2005; 24:208–218. [PubMed: 15896949]
48. Karp JM, Sarraf F, Shoichet MS, Davies JE. Fibrin-filled scaffolds for bone-tissue engineering: An in vivo study. J Biomed Mater Res Part A. 2004; 71A:162–171.
49. Le Nihouannen D, Guehennec LL, Rouillon T, Pilet P, Bilban M, Layrolle P, et al. Micro-architecture of calcium phosphate granules and fibrin glue composites for bone tissue engineering. Biomaterials. 2006; 27:2716–2722. [PubMed: 16378638]
50. Peled E, Boss J, Bejar J, Zinman C, Seliktar D. A novel poly(ethylene glycol)–fibrinogen hydrogel for tibial segmental defect repair in a rat model. J Biomed Mater Res Part A. 2007; 80A:874–884.
51. Mulliken JB, Kaban LB, Glowacki J. Induced osteogenesis—The biological principle and clinical applications. Journal of Surgical Research. 1984; 37:487–496. [PubMed: 6392745]
52. Schlag G, Redl H. Fibrin sealant in orthopedic surgery. Clin Orthop Relat Res. 1988; 227:269–285. [PubMed: 2448076]
53. Le Guehennec L, Layrolle P, Daculsi G. A review of bioceramics and fibrin sealant. Eur Cell Mater. 2004; 8:1–10. discussion-1. [PubMed: 15494929]
54. Abiraman S, Varma HK, Umashankar PR, John A. Fibrin glue as an osteoinductive protein in a mouse model. Biomaterials. 2002; 23:3023–3031. [PubMed: 12069345]
55. Kania RE, Meunier A, Hamadouche M, Sedel L, Petite H. Addition of fibrin sealant to ceramic promotes bone repair: long-term study in rabbit femoral defect model. J Biomed Mater Res. 1998; 43:38–45. [PubMed: 9509342]
56. Karp JM, Sarraf F, Shoichet MS, Davies JE. Fibrin-filled scaffolds for bone-tissue engineering: An in vivo study. J Biomed Mater Res A. 2004; 71:162–171. [PubMed: 15368266]
57. Bensaid W, Triffitt JT, Blanchat C, Oudina K, Sedel L, Petite H. A biodegradable fibrin scaffold for mesenchymal stem cell transplantation. Biomaterials. 2003; 24:2497–2502. [PubMed: 12695076]

58. Cunin G, Boissonnet H, Petite H, Blanchat C, Guillemin G. Experimental vertebroplasty using osteoconductive granular material. Spine (Phila Pa. 1976; 25:1070–1076.

59. Connelly JT, García AJ, Levenston ME. Inhibition of in vitro chondrogenesis in RGD-modified three-dimensional alginate gels. Biomaterials. 2007; 28:1071–1083. [PubMed: 17123602]

60. Shih Y-RV, Tseng K-F, Lai H-Y, Lin C-H, Lee OK. Matrix stiffness regulation of integrin-mediated mechanotransduction during osteogenic differentiation of human mesenchymal stem cells. Journal of Bone and Mineral Research. 2011; 26:730–738. [PubMed: 20939067]

61. Gronthos S, Simmons PJ, Graves SE, Robey PG. Integrin-mediated interactions between human bone marrow stromal precursor cells and the extracellular matrix. Bone. 2001; 28:174–181. [PubMed: 11182375]

62. Lossdörfer S, Schwartz Z, Wang L, Lohmann CH, Turner JD, Wieland M, et al. Microrough implant surface topographies increase osteogenesis by reducing osteoclast formation and activity. J Biomed Mater Res Part A. 2004; 70A:361–369.

63. Balloni S, Calvi EM, Damiani F, Bistoni G, Calvitti M, Locci P, et al. Effects of titanium surface roughness on mesenchymal stem cell commitment and differentiation signaling. Int J Oral Maxillofac Implants. 2009; 24:627–635. [PubMed: 19885402]

64. Chastain SR, Kundu AK, Dhar S, Calvert JW, Putnam AJ. Adhesion of mesenchymal stem cells to polymer scaffolds occurs via distinct ECM ligands and controls their osteogenic differentiation. J Biomed Mater Res. 2006; 78A:73–85.

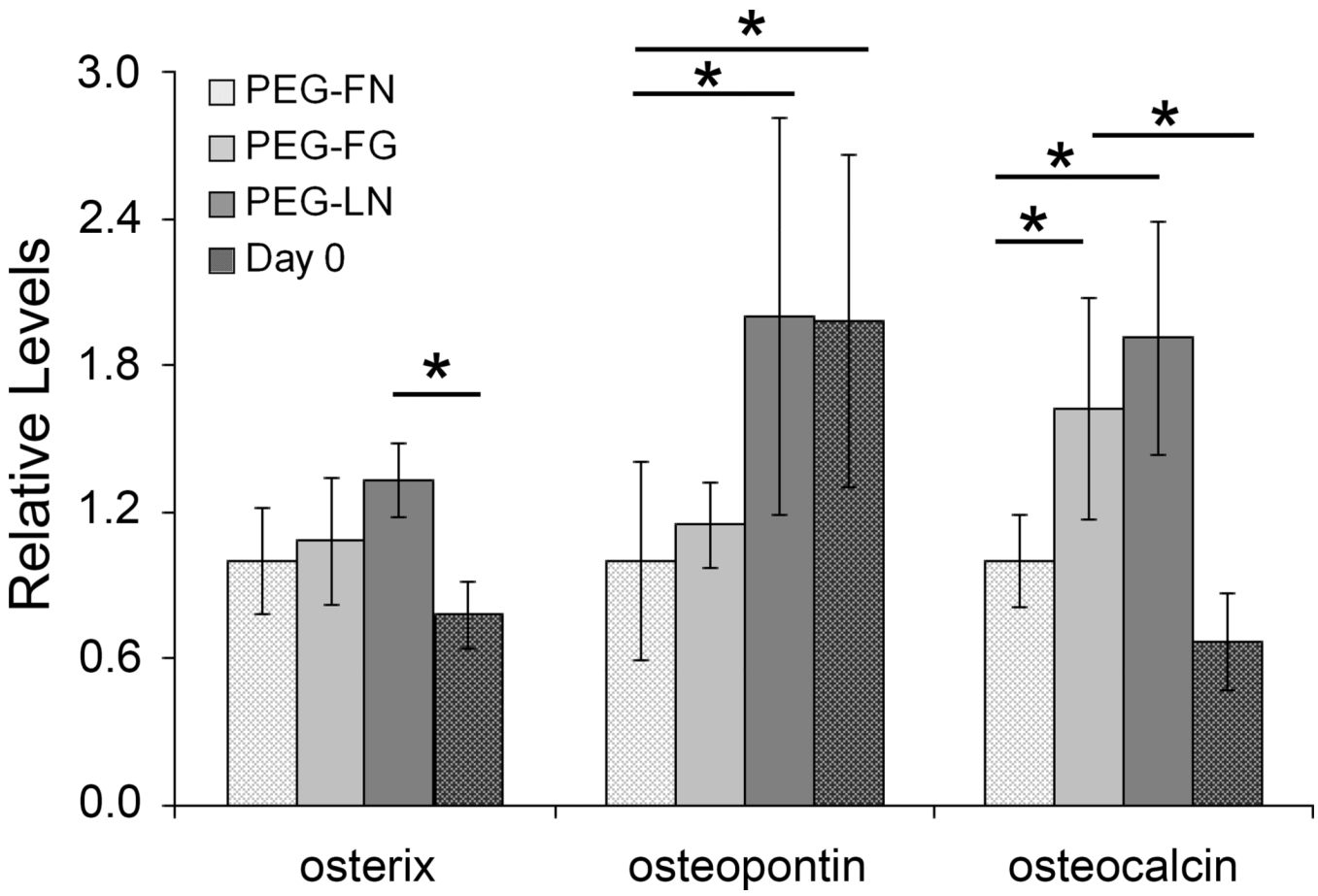

Figure 1.

Expression of osteogenic markers osterix, osteopontin, and osteocalcin by ELISA (osterix and osteocalcin) and cell counts (osteopontin). For ELISA assays, 6 samples per day 7 formulation were analyzed. The day 0 ELISA sample number was n = 4. For cell counts, sections from 4–8 separate samples of each formulation were evaluated. Validation of the cell counting assessment method is given in Supplementary Figure 3. For the purpose of comparison, ELISA and cell count measures for each protein have been normalized to the corresponding measure for PEG-FN gels. * indicates a significant difference, $p < 0.05$.

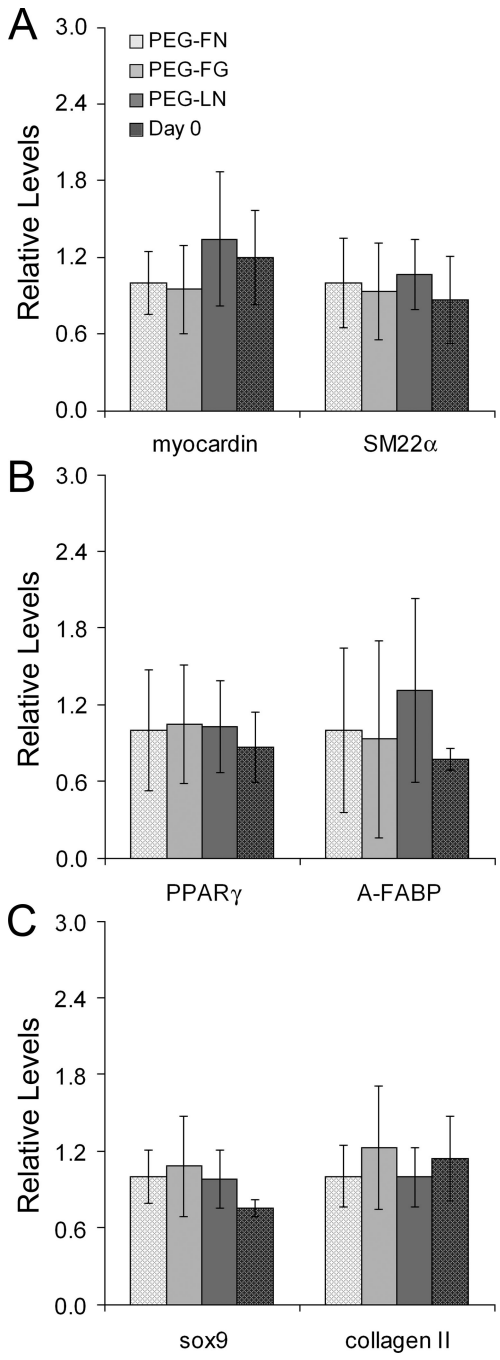

Figure 2.

(A) Expression of myocardin and SM22α, as assessed by cell counting and ELISA methods, respectively. (B) Expression of PPAR and A-FABP, as assessed by cell counting and ELISA methods, respectively. (C) Expression of sox9 and collagen II by ELISA. For ELISA assays, 6–9 samples per day 7 formulation were analyzed. The day 0 ELISA sample number was n = 4. For cell counts, sections from 4 separate discs of each formulation were evaluated. For the purpose of comparison, ELISA and cell count measures for each protein have been normalized to the corresponding measure for PEG-FN gels.

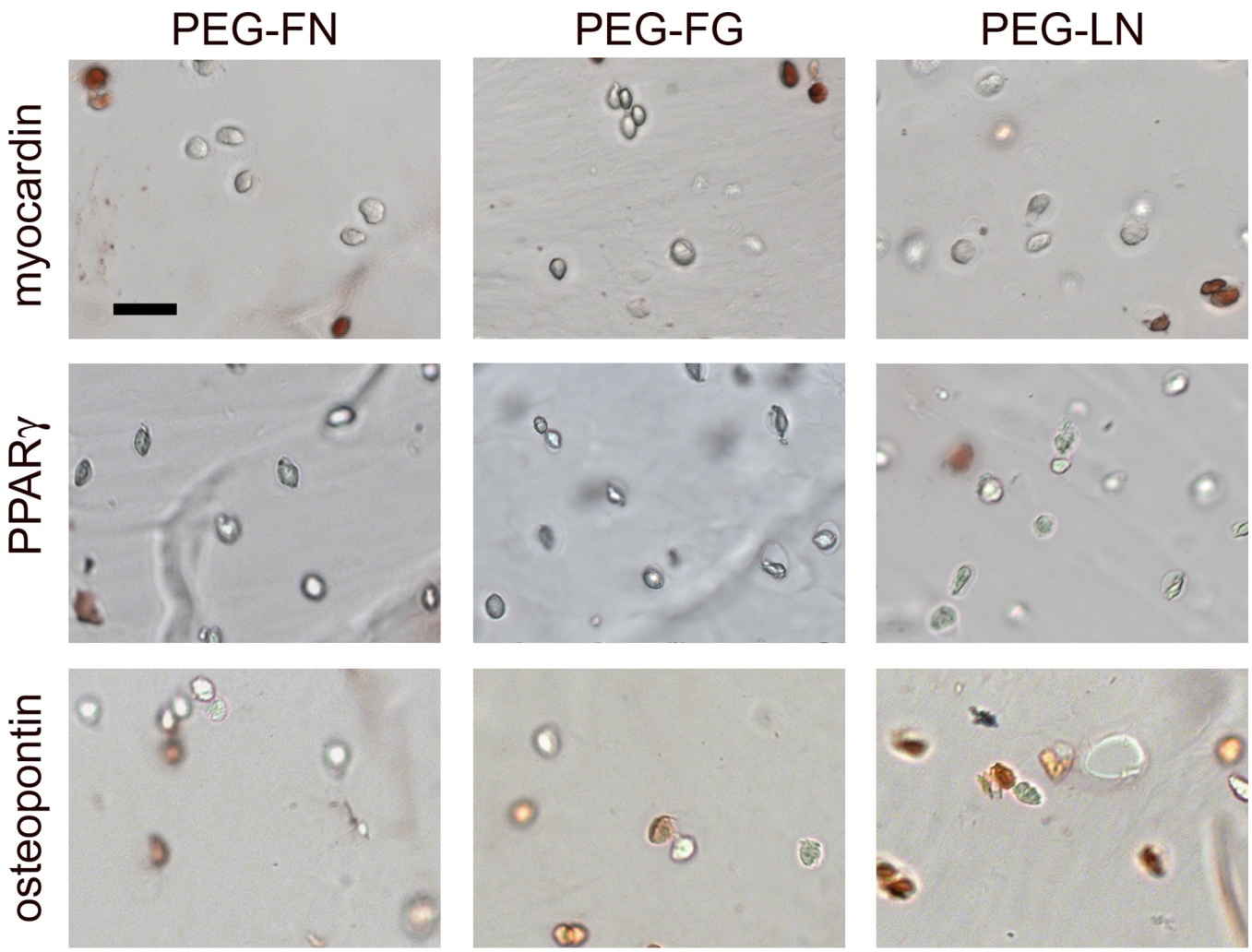

Figure 3.
Representative images of day 7 immunostaining for myocardin, PPAR, and osteopontin. Positive staining is indicated by brown (PPAR and osteopontin) or red (myocardin) coloration. Scale bar = 40 μm and applies to all images.

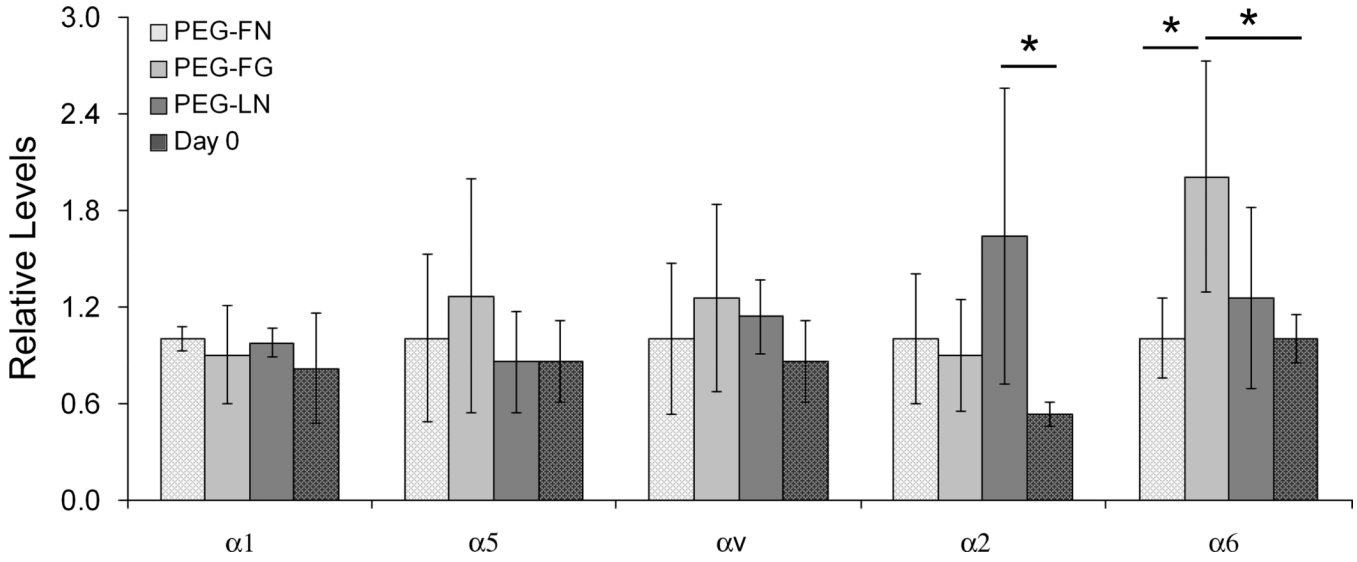

Figure 4.

Day 7 and day 0 expression of various integrin alpha subunits as assessed by ELISA (n = 6–9 per day 7 formulation; n = 4 for day 0). For the purpose of comparison, ELISA measures for each protein have been normalized to the corresponding measure for PEG-FN gels. * indicates a significant difference, $p < 0.05$.

Table 1

Comparison of the average modulus and mesh size of 8 mm discs of each PEG-ECM hydrogel formulation with time in culture[†]

Gel Type	Modulus (kPa)		Mesh Size (μg dextran/g gel)	
	Day 0	Day 7	Day 0	Day 7
PEG-FN	33.3 ± 0.7	29.2 ± 0.8[*]	11.8 ± 0.3	12.4 ± 0.3
PEG-FG	33.9 ± 1.9	29.9 ± 1.5[*]	11.4 ± 0.3	11.7 ± 0.2
PEG-LN	33.7 ± 2.0	28.7 ± 1.2[*]	11.6 ± 0.3	11.8 ± 0.6

[†]Property results represent an average of n = 4 samples for each PEG-ECM formulation.

[*]Significantly different from the corresponding day 0 value, $p < 0.05$

Table 2

Comparison of the average thickness, mass, and cell density in discs of each PEG-ECM hydrogel formulation with time in culture[†]

Gel Type	Thickness (mm)		Mass of 8 mm Discs (mg)		Cell Density (×10^6)	
	Day 0	Day 7	Day 0	Day 7	Day 0	Day 7
PEG-FN	0.55 ± 0.01	0.56 ± 0.01	29.1 ± 0.2	29.5 ± 0.2	1.01 ± 0.06	0.88 ± 0.08[*]
PEG-FG	0.55 ± 0.01	0.56 ± 0.01	29.2 ± 0.2	29.4 ± 0.5	0.96 ± 0.05	0.74 ± 0.02[*]
PEG-LN	0.54 ± 0.01	0.56 ± 0.01	29.2 ± 0.4	29.3 ± 0.3	1.02 ± 0.02	0.82 ± 0.02[*]

[†]Results represent an average of n = 4 samples for each PEG-ECM formulation.

[*]Significantly different from the corresponding day 0 value, $p < 0.05$

Table 3

Percent inhibition of 10T½ cell adhesion at day 0 by blocking antibodies to various integrin alpha subunits[†]

Gel Type	α_1	α_2	α_v	α_5	α_6
PEG-FN	--	31.9 ± 26.5	52.9 ± 22.8	15.2 ± 5.0	--
PEG-FG	--	-- [*]	97.5 ± 8.7 [*]	2.4 ± 7.7 [*]	--
PEG-LN	31.7 ± 10.7 [*,#]	-- [*]	24.9 ± 9.6 [#]	26.4 ± 5.9 [*,#]	17.0 ± 7.8 [*,#]

[†] Integrin inhibition results represent an average of n = 5–10 sample wells per antibody per ECM molecule

-- indicates no inhibition detected

[*] Significantly different from the corresponding PEG-FN gels, $p < 0.05$

[#] Significantly different from the corresponding PEG-FG gels, $p < 0.05$